Asian Journal of Information Technology 15 (1): 82-89, 2016
ISSN: 1682-3915
© Medwell Journals, 2016

Removal of Motion Blur Through Markov Random Field Model

[1]J. Amudha and [2]R. Sudhakar
[1]Department of Electrical and Electronics Engineering,
[2]Department of Electronics and Communication Engineering,
Dr. Mahalingam College of Engineering and Technology, 642003 Pollachi, Tamil Nadu, India

Abstract: This research study focuses on restoring images that are affected by motion blur which corrupts the image during acquisition. Restoration of images is an ill problem in image processing. A model derived from Markov Random Fields (MRF) is proposed to remove blur iteratively followed by best fit selector. Even then the blur components will be present in low frequencies. To reduce low frequency blur components, Discrete Wavelet Transform (DWT) is used and a second stage of MRF deblurring is done before the wavelet synthesis procedure. Experimental results shows better performance of the projected deblurring algorithm compared to other techniques in terms of image quality measures.

Key words: Deblurring, image restoration, Markov random field, motion blur, multi-resolution, wavelet transform

INTRODUCTION

Restoration of image is a significant concern in advanced image processing. Images are frequently degraded at some stage of data acquisition procedure. The degradation may possibly involve blurring, detail loss owing to sampling, quantization property and a variety of sources of noise. Image deblurring plays an essential role in several image processing applications. The aspiration of image deblurring is to get better sharp image from a blurry surveillance. Blur is an outward appearance of reduction in bandwidth of the image due to defective image development procedure. It may be because of relative motion between capturing device and the original image. In general, an image may be corrupted by means of low-pass filters as they are accustomed to blur or smooth the image.

Various approaches have been projected to deblur a noisy image. The overall computation of modified wiener filter (Xu *et al*., 2011) was carried out in the frequency domain using Fast Fourier Transform (FFT) and the circulant matrix approximation for randomly blurred images. Richardson-Lucy Algorithm with total variation regularization (Dey *et al*., 2006) for 3D confocal microscope deconvolution suppresses the unstable oscillations without affecting object edges. Comparison of two methods (Bojarczak and Lukasik, 2007) namely Wiener filter, where the noise variance was involved in blurring process as a known priori and Truncated Singular Value Decomposition (TSVD) in which the knowledge of precise noise variance is not required to renovate the image, reveals that Wiener filter provides better results. An Adaptively Accelerated Lucy-Richardson (AALR) method for image deblurring (Singh *et al*., 2008) employs an empirical technique that calculates the corrective exponent in all iterations in an adaptive way by first order derivative of the restored image in the last two iterations.

A blind motion deblurring technique using sparse approximation (Cai *et al*., 2009) removes the motion blur in a single image by inventing the blind motion blurring as a joint optimization crisis that concurrently maximizes the sparsity of the blur kernel and the sparsity of the apparent image under appropriate redundant tight frame systems. A regularization based approach requires no prior information of the blur kernel (Cai *et al*., 2012) to remove the motion blur in an image by regularizing the sparsity of mutually the original image and the motion-blur kernel under tight wavelet frame systems. A modified description of the split Bregman technique is also introduced to work out the resultant minimization problem efficiently. Sparse Representation (SR) based blind image deblurring (Zhang *et al*., 2011) develops the sparsity prior of original images that helps in improves the ill-posed problem. The undesirable ringing artifacts and noise amplifications are less in the restored image due to the incorporation of sparsity regularization.

Deblurring of gray scale images using inverse and Wiener Filter (Sankhe *et al*., 2011) used the inverse filters for pre-correcting an input signal in anticipation of the

Corresponding Author: J. Amudha, Department of Electrical and Electronics Engineering,
Dr. Mahalingam College of Engineering and Technology, 642003 Pollachi, Tamil Nadu, India

degradations caused by the system and Wiener filter to minimize the mean squared restoration error which is the existing disparity between the original and restored images. The power of Markov Random Field (MRF) models in modeling an image fusion problem (Xu *et al*., 2011) was investigated and the association of each source image and the true image was established. Modified Lucy Richardson Algorithm (Sharma *et al*., 2013) utilised DWT as pre-processing stage of image restoration in the presence of Gaussian blur and motion blur and then Lucy-Richardson algorithm was applied.

Overview of de-blurring: The goal of image deblurring is to recover a sharp image from blurry observation. Blur portrays the fact that information fit in to a single object point is smeared over a definite region in the image as an alternative to be sharply localized. Smear is unsharp image vicinity sourced by means of camera or incorrect focus. The smear effects are filters that average the changeovers and diminish the disparity by smoothing the pixels after the firm boundaries of distinct lines and regions of significant color evolution.

In accordance with physical conditions blur is classified into out of focus blur, motion blur and atmospheric turbulence blur. Divergence of an imaging plane from the focal point of lens causes out of focus blur. Motion blur is attributable to relative motion relating capturing device and its targeted object. When an object or the image capturing gadget is moved at some stage in light exposure a motion blurred image is formed. Atmospheric blur is owing to spreading of photonic media during which light rays travel. Techniques that can diminish the blur and thus improving the version of blurred images are named as deconvolution or deblurring. However, deblurring is a highly ill-posed problem modelled as shown in Fig. 1. The motion blur effect is created by a filter so as to produce the image appeared to be stirring by additive blur in an unambiguous direction. The motion blur can be illicit by a distance or by an angle in either side and or intensity in pixels. A deblurred or corrupted image can be estimated described by this equation:

$$g(x,y) = h(x,y) \times f(x,y) + \eta(x,y) \quad (1)$$

Where:

- g(x,y) = The blurred image
- h(x,y) = The degrading operator which is known as Point Spread Function (PSF)
- f (x,y) = The original image and
- η(x,y) = Additive noise that may originated during the image capturing process which damages the image PSF
- h (x,y) = The degree of which an optical system blurs a point of light

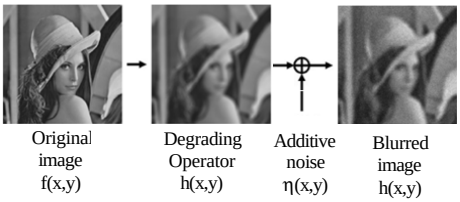

Fig. 1: Data model for deblurring problem

The Optical Transfer Function (OTF) is the impulse response of a linear, position-invariant system and it is the Fourier transform of PSF. Image deblurring is an inverse problem that is used to improve an image experienced linear degradation. The degradation may be space invariant or space variant. Blurring is the convolution of the PSF and the original image, in the spatial invariant system and hence, image deblurring is equal to image deconvolution, i.e., the inverse processing of convolution. Several methods have been established for the past several decades. Wiener filter is one of the frequency domain method of recovering the image in the presence of blur and noise which uses casual and anti casual procedure to wipe out the blurring effect in an affected image (Tekalp *et al*., 1992; Buades *et al*., 2005). Regulated filter is another effective method of deblurring an image using deconvergence of the deconvolution function, which is effective when the partial information about additive noise is known (Al-Amri and Kalyankar, 2010).

MRF has added advantage to the efforts in sustaining image's detail. Its flexibility enhances its use in image classification (Tso and Mather, 1999; Niu and Ban, 2012), segmentation (Deng and Clausi, 2004; Yang and Clausi, 2012; Zheng *et al*., 2011; You *et al*., 2014), cloud detection (Addesso *et al*., 2012) and change detection (Bruzzone and Prieto, 2000, 2002; Kasetkasem and Varshney, 2002). Moreover, the use of MRF in reducing the effect of speckle noise is envisaged in contextual information modeling (Moser *et al*., 2007; Moser and Serpico, 2009).

MATERIALS AND METHODS

Proposed de-blurring algorithm

MRF: MRF (Li, 2009) is undirected graphical representation, in which the random variable in it follows Markov property. This MRF have turn out to be quite a good algorithm in adapting image related processing such as computer vision and statistical pattern recognition, image segmentation, image compression, tomography reconstruction, etc. MRF concentrates on the intensity sharing of an image in which the texture categorization is done. This texture categorization shows the different objects present in an image through which their edge was

found like segmentation. From this segmentation, the PSF was originated to suppress the low frequency consequence and also to enhance the boosting of high frequency/sharpness.

Each pixel in an image can be considered as a random variable. An image can be described as the realization of an N X M dimensional random variable of Probability Density Function (PDF). Given the detail that N and M are the dimensions of the image, each component of the vector represents a pixel in the image. This is called a random field. The sample p(X) to generate a sample image from a given random field where X is the N X M random field. Assuming that all the pixels are uncorrelated and can be model p(X) as:

$$p(X)=\prod_{i=1}^{n} p(x_i) \tag{2}$$

where, x_i are the pixels of the image. To commence correlation in its general form and need to suppose that all the pixels in the image are correlated and reflect on all the pixels simultaneously. This is impossible in performing because of the size of the sampling space (2^{NM} for a binary image, k^{NM} for a k grey level image). If assumed that a pixel depends only on its neighbors, the random field is called as MRF. To a great extent it is easier to consider change in one pixel in the image only affects its neighbors. A random field is a MRF if P(X = x) has a Gibbs distribution and P(X) is articulated as:

$$P(X=x)=\frac{1}{Z}e^{-\frac{1}{T}U(x)} \tag{3}$$

The Hidden Markov models (HMM) are the mainly used prior models for state variables X_i that are to be inferred from a related set of observations or measurements $z = (z_1, z_2, ..., z_i, ..., z_N)$. The measurements z that are instantaneously considered of a random variable Z, where z_i represents the spectral content of a part of an image signal and Xi represents a state in time domain. It leads to an implication problem in possible states X, from the observations z, is calculated using Bayes's formula as $P(X = x|Z = z) \propto P(Z = z|X = x)P(X = x)$. Here, P (X = x) is the prior distribution over states. The skip over constant of proportionality would be the best to fix that $\sum_x P(x|z) = 1$. When multiple models are simultaneously taken into account, it is denoted as $P(x|z, \omega) \propto P(z|x, \omega)P(x|\omega)$, The constant of proportionality in this relation will depends on ω and z. The Markov chain is used to represent the prior of a HMM and it can be decomposed as a product of conditional distributions. P (z|x) is the likelihood parameter that is observed from the experiment which is used to keep the blurring removal process under control in-order to reduce the damage caused to the image information. SSIM is used for measuring the quality of the image and how much it is blur free. The more the likelihood will be compacted into a single fine peak.

Problem formulation: Let us consider an image X of size M X N, it can be modeled as:

$$P(X=x)=\frac{1}{Z}e^{-\frac{1}{T}U(x)} \tag{4}$$

Where:

Z = Normalizing Constant
U(x) = Prior energy and
T = Control parameter called Temperature

Gibbs distribution is acceptable by the following reasons. The Hamersley-Clifford theorem (Li, 2009) states that any conditional distribution has a joint distribution which is Gibbs distribution if the below mentioned conditions hold good:

- Positivity: $P(X = x)>0$
- Locality $P(X_s = x_s|X_t = x_t, t\neq s, t\epsilon s) = P(X_s = x_s|X_t = x_t, t\neq s, t\epsilon G_s)$
- Homogeneity: $P(X_s= x_s|X_t= x_t, t\neq s, t\epsilon G_s)$ is similar to all sites s

MRF modeling has some well-built reasons to be used is as follows:

- A systematical problem solving methodology for the different dataset
- It characterizes the quantitative performance measures in an effective way
- It is capable of incorporating many contextual information of a dataset
- This MRF algorithm is adaptable to hardware based systems

The projected method recovers the image in three phases. The Phase-I is pre processing step in which the blurred input image is resized and blind deconvolution is done based on initial PSF. Then first level of MRF deblurring is done iteratively in Phase-II followed by best descriptor process to select the optimal image. This image will have some boundary value mismatch in its low frequency components. So, the optimal image is allowed to undergo level 1 Wavelet analysis and then second level of MRF deblurring to remove the remaining blur effect before the image is recovered by wavelet synthesis in Phase III (Fig. 2).

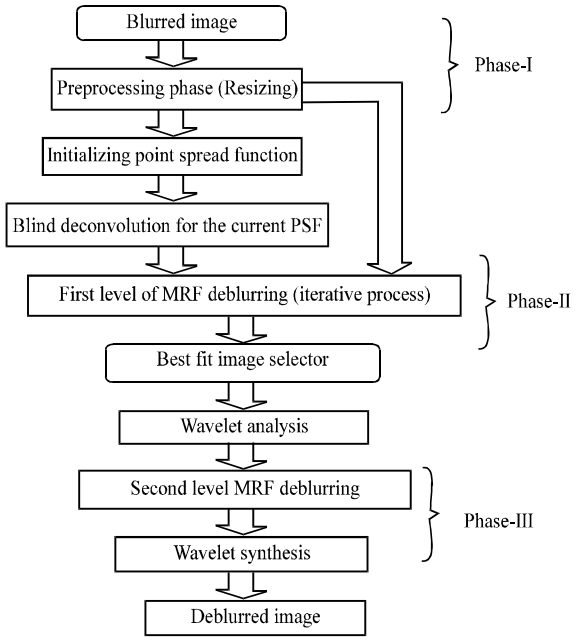

Fig. 2: Schematic flow chart of proposed method

Fig. 3: Restored images obtained from synthesized images with blur lengths L = 8, 12, 18, 21, respectively by: a) Wiener filter; b) LR method; c) Proposed method

RESULTS AND DISCUSSION

This study evaluates the de-blurring effect in terms of Peak Signal-to-Noise Ratio (PSNR), Mean Square Error (MSE) to compare with other methods:

$$PSNR = 10\log_{10}(255^2/MSE) \quad (5)$$

$$MSE = \frac{1}{M \times N}\sum_{i=0}^{M-1}\sum_{j=0}^{N-1}\left(f^{*}_{i,j} - f_{i,j}\right) \quad (6)$$

The proposed method is tested and compared with Wiener filtering method and Lucy Richardson (LR) method. First, it was synthesized some sample motion blurred images generated on a range of standard gray-scale test images with specifically different features and different sizes. Experiments are carried out on those images and following measures like Signal to Noise ratio (SNR), Peak Signal to Noise ratio (PSNR), Image Fidelity (IF), Average Absolute Difference (AAD), Mean Square error (MSE), Correlation Co-efficient (CC) and Structural Similarity (SSIM) are used to assess the quantitative performance. The test image chosen is camera man image of size 256×256. Camera man image was synthesized with various blur lengths and restored by Wiener filtering, LR method and proposed method. Figure 3a-c represent the output images processed by Wiener filtering, LR

algorithm and the proposed algorithm for blur lengths L = 8, 12, 18 and 21, respectively. Table 1 summarizes the performance of the suggested method at several blur lengths for various synthesized images of size 256×256. Figure 4a-c shows the original Camera man image, synthesized input image with blur length L = 21 and the restored images processed by Wiener filtering, LR algorithm and proposed method. Figure 5 and 6 shows

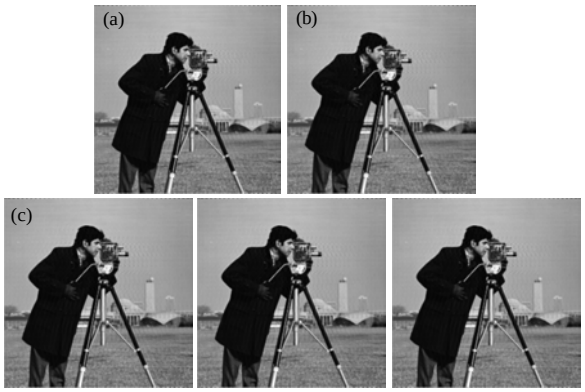

Fig. 4: a) Original image; b) Synthesized image degraded by motion blur with L = 21; c) Restored images obtained by Wiener Filter, LR method and Proposed method, respectively

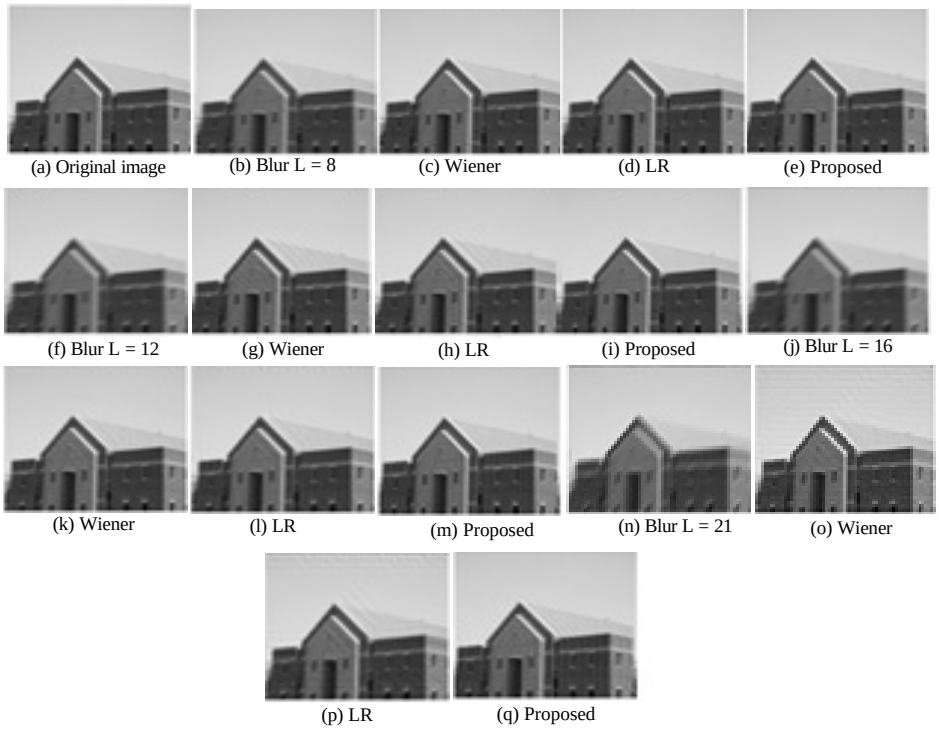

Fig. 5: House image

Table 1: Comparison of performance measures of proposed method with Wiener filter and LR method

Image		House				Flower				Cameraman			
Blur length		L = 8	L = 12	L = 16	L = 21	L = 8	L = 12	L = 16	L = 21	L = 8	L = 12	L = 16	L=21
SNR(dB)	Weiner	22.26	21.84	21.59	21.20	21.59	20.66	20.37	19.76	14.56	13.94	13.44	12.91
	LR	23.67	23.18	21.59	20.89	24.01	21.67	20.37	19.63	16.36	14.71	13.76	12.80
	Proposed	25.31	24.11	23.48	23.35	23.68	22.92	22.36	22.45	18.20	17.39	16.64	14.74

Table 1: Continue

Image		House				Flower				Cameraman			
Blur length		L = 8	L = 12	L = 16	L = 21	L = 8	L = 12	L = 16	L = 21	L = 8	L = 12	L = 16	L=21
PSNR(dB)	Weiner	26.58	26.15	25.90	25.51	25.43	24.50	24.21	23.60	20.08	19.46	18.96	18.42
	LR	27.98	27.49	25.90	25.20	27.86	25.51	24.21	23.47	21.88	20.22	19.28	18.32
	Proposed	28.36	27.17	26.55	26.43	26.45	25.70	25.16	25.26	23.20	22.30	21.69	19.88
IF	Weiner	-0.006	-0.007	-0.007	-0.008	-0.007	-0.009	-0.009	-0.011	-0.035	-0.040	-0.048	-0.051
	LR	-0.004	-0.005	-0.007	-0.008	-0.004	-0.007	-0.009	-0.011	-0.023	-0.034	-0.042	-0.052
	Proposed	-0.003	-0.005	-0.005	-0.005	-0.005	-0.006	-0.007	-0.007	-0.020	-0.023	-0.080	-0.044
MSE	Weiner	143	157	167	182	186	230	246	283	637	735	825	933
	LR	103	116	167	196	106	182	246	292	420	616	766	956
	Proposed	95	124	143	148	147	175	198	193	311	382	440	667
AAD	Weiner	0.039	0.041	0.042	0.044	0.048	0.053	0.055	0.060	0.078	0.083	0.087	0.093
	LR	0.032	0.034	0.042	0.046	0.035	0.047	0.055	0.061	0.039	0.050	0.041	0.041
	Proposed	0.082	0.096	0.102	0.108	0.138	0.150	0.159	0.159	0.012	0.014	0.016	0.016
CC	Weiner	0.974	0.951	0.938	0.920	0.907	0.893	0.873	0.824	0.966	0.944	0.921	0.896
	LR	0.965	0.932	0.916	0.904	0.870	0.836	0.807	0.791	0.947	0.902	0.894	0.784
	Proposed	0.965	0.960	0.944	0.934	0.909	0.909	0.893	0.890	0.924	0.896	0.865	0.835
SSIM	Weiner	0.803	0.701	0.696	0.683	0.401	0.370	0.357	0.321	0.672	0.644	0.583	0.547
	LR	0.783	0.641	0.621	0.601	0.374	0.313	0.294	0.284	0.544	0.424	0.416	0.389
	Proposed	0.792	0.710	0.699	0.692	0.408	0.409	0.381	0.380	0.574	0.456	0.399	0.270

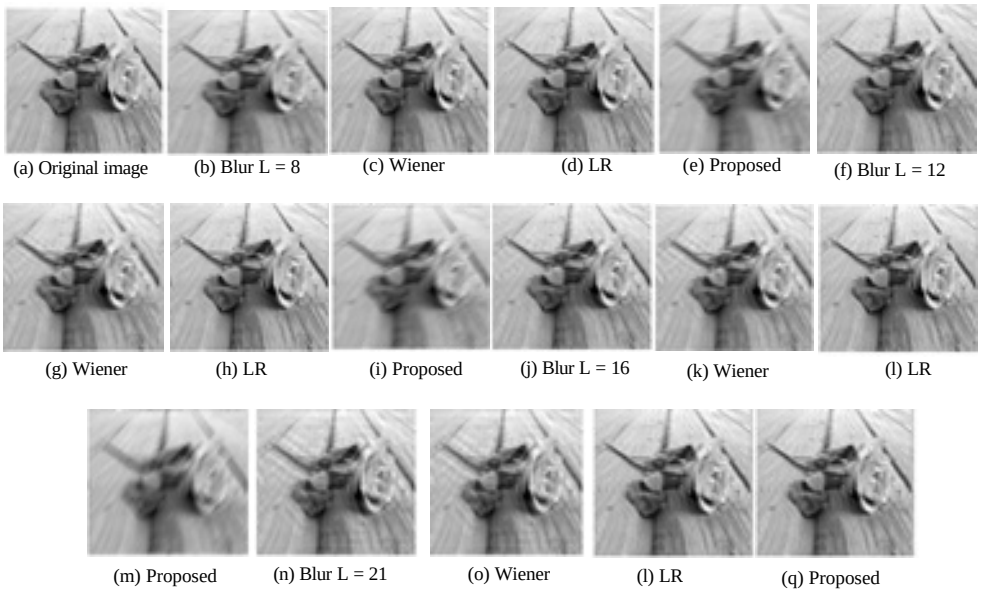

Fig. 6: Flower image

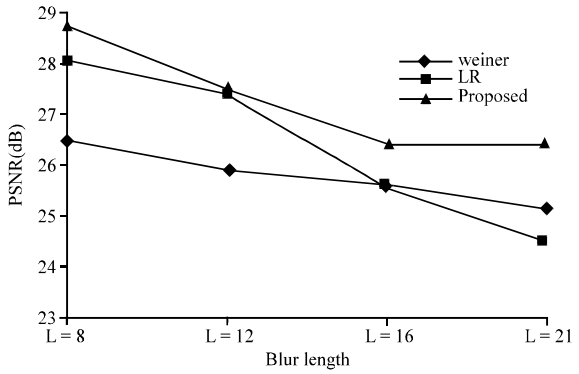

Fig. 7: Comparison of PSNR of various methods; house image PSNR vs blur length

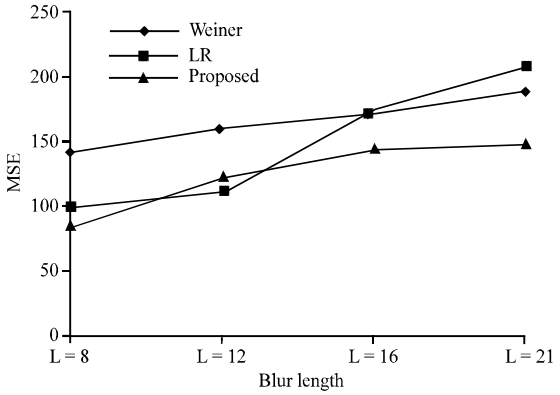

Fig. 8: Comparison of MSE of various methods; house image PSNR vs blur length

that the proposed method seems to be visually good and superior to other methods. The PSNR curves and MSE curves for various blur lengths of house image were measured and plotted in Fig. 7 and 8, respectively.

CONCLUSION

The proposed research exhibits a new deblurring algorithm using MRF modeling to deblur an image with varying blur lengths. This method solves the effect of blurring by analyzing the image from spectral point of view using SSIM. By means of iterative analysis the continuous correction for the image has been made with measuring the image quality. Experimental evaluation of the projected algorithm is done on synthesized motion blurred images obtained from standard test images and the results demonstrate better performance of the proposed algorithm irrespective of nature of input. It is clear from the results that the suggested method is superior among all methods and is simple and effective.

REFERENCES

Addesso, P., R. Conte, M. Longo, R. Restaino and G. Vivone, 2012. MAP-MRF cloud detection based on PHD filtering. Sel. Top. Appl. Earth Obs. Remote Sens. IEEE. J., 5: 919-929.

Al-Amri, S.S. and N.V. Kalyankar, 2010. A comparative study for deblured average blurred images. Int. J. Comput. Sci. Eng., 2: 731-733.

Bojarczak, P. and Z. Lukasik, 2007. Image deblurring-wiener filter versus TSVD approach. Adv. Electr. Electron. Eng., 6: 86-89.

Bruzzone, L. and D.F. Prieto, 2000. Automatic analysis of the difference image for unsupervised change detection. Geosci. Remote Sens. IEEE. Trans., 38: 1171-1182.

Bruzzone, L. and D.F. Prieto, 2002. An adaptive semiparametric and context-based approach to unsupervised change detection in multitemporal remote-sensing images. Image Process. IEEE. Trans., 11: 452-466.

Buades, A., B. Coll and J.M. Morel, 2005. A non-local algorithm for image denoising. Proceedings of the 2005 IEEE Computer Society Conference on Computer Vision and Pattern Recognition, June 20-26 IEEE Computer Society, USA., pp: 60-65.

Cai, J.F., H. Ji, C. Liu and Z. Shen, 2009. Blind motion deblurring from a single image using sparse approximation. Proceedings of the Conference on Computer Vision and Pattern Recognition, June 20-25, 2009, Miami, FL., pp: 104-111.

Cai, J.F., H. Ji, C. Liu and Z. Shen, 2012. Framelet-based blind motion deblurring from a single image. Image Process. IEEE. Trans., 21: 562-572.

Deng, H. and D.A. Clausi, 2004. Unsupervised image segmentation using a simple MRF model with a new implementation scheme. Pattern Recognit., 37: 2323-2335.

Dey, N., L.B. Feraud, C. Zimmer, P. Roux and Z. Kam *et al.*, 2006. Richardson-lucy algorithm with total variation regularization for 3D confocal microscope deconvolution. Microsc. Res. Tech., 69: 260-266.

Kasetkasem, T. and P.K. Varshney, 2002. An image change detection algorithm based on Markov random field models. Geosci. Remote Sens. IEEE. Trans., 40: 1815-1823.

Li, S.Z., 2009. Markov Random Field Modeling in Image Analysis. 3rd Edn., Springer, Heidelberg, ISBN: 9781848002784, pp: 74-76.

Moser, G. and S.B. Serpico, 2009. Unsupervised change detection from multichannel SAR data by Markovian data fusion. Geosci. Remote Sens. IEEE. Trans., 47: 2114-2128.

Moser, G., S. Serpico and G. Vernazza, 2007. Unsupervised change detection from multichannel SAR images. Geosci. Remote Sens. Lett. IEEE., 4: 278-282.

Niu, X. and Y. Ban, 2012. An adaptive contextual SEM algorithm for urban land cover mapping using multitemporal high-resolution polarimetric SAR data. Appl. Earth Obs. Remote Sens. IEEE. J., 5: 1129-1139.

Sankhe, P.D., M. Patil and M. Margaret, 2011. Deblurring of grayscale images using inverse and Wiener filter. Proceedings of the International Conference and Workshop on Emerging Trends in Technology, February 25-26, 2011, ACM, Mumbai, Maharashtra, India, ISBN: 978-1-4503-0449-8, pp: 145-148.

Sharma, S., S. Sharma and R. Mehra, 2013. Image restoration using modified lucy richardson algorithm in the presence of Gaussian and Motion Blur. Adv. Electron. Electr. Eng., 3: 1063-1070.

Singh, M.K., U.S. Tiwary and Y.H. Kim, 2008. An adaptively accelerated lucy-richardson method for image deblurring. EURASIP. J. Adv. Signal Process., 365021: 1-10.

Tekalp, A.M., M.K. Ozkan and M.I. Sezan, 1992. High-resolution image reconstruction from lower-resolution image sequences and space-varying image restoration. Proceeding of the IEEE International Conference on Acoustics, Speech and Signal Processing, ICASSP-92., 1992, March 23-26, 1992, IEEE, San Francisco, CA., pp: 169-172.

Tso, B.C. and P.M. Mather, 1999. Classification of multisource remote sensing imagery using a genetic algorithm and Markov random fields. Geosci. Remote Sens. IEEE. Trans., 37: 1255-1260.

Xu, M., H. Chen and P.K. Varshney, 2011. An image fusion approach based on Markov random fields. Geosci. Remote Sens. IEEE. Trans., 49: 5116-5127.

Yang, X. and D.A. Clausi, 2012. Evaluating SAR sea ice image segmentation sing edge-preserving region-based MRFs. Sel. Top. Appl. Earth Obs. Remote Sens. IEEE. J., 5: 1383-1393.

You, D., S. Antani, D.D. Fushman and G.R. Thoma, 2014. An MRF model for biomedical image segmentation. Proceeding of the IEEE 27th International Symposium on Computer-Based Medical Systems (CBMS), 2014, May 27-29, 2014, IEEE, New York, USA., pp: 539-540.

Zheng, C., L. Wang, Y. Hu and Q. Qin, 2011. Region-based MRF model with optimized initial regions for image segmentation. Proceeding of the 2011 International Conference on Remote Sensing, Environment and Transportation Engineering (RSETE), June 24-26, 2011, IEEE, Nanjing, China, pp: 3354-3357.